WebLog Journal of Dentistry and Oral Disorders

Research Article
Published: 11 Jun, 2026

Association of Cone Beam CT Texture Parameters with Mandibular Bone Density and Structural Disorganization in Postmenopausal Women

Andrezza Pires da Rocha Carvalho[1], Gabriela Franco da Rosa Caetano[2]*, André Luiz Ferreira Costa[3], Márcia Oliveira de Carvalho[4], Kelmara Arruda Pinho[1], José Luiz Cintra Junqueira[1], Marcelo Gusmão Paraiso Cavalcanti[2] and Francine Kühl Panzarella[1]

[1]Division of Oral Radiology, São Leopoldo Mandic Faculty, São Leopoldo Mandic Research Institute, Campinas, São Paulo, Brazil

[2]Division of Oral and Maxillofacial Radiology, Department of Stomatology, School of Dentistry, University of São Paulo, São Paulo (SP), Brazil

[3]Postgraduate Program in Dentistry, Dentomaxillofacial Radiology and Imaging Laboratory, Cruzeiro do Sul University (UNICSUL), São Paulo, Brazil

[4]Department of Physics, Institute of Exact Sciences and Technology, University of Campinas – UNICAMP, Jundiaí, Brazil

WebLog Open Access Publications
Article ID : wjdod.2026.f1105
Author : Gabriela Franco da Rosa Caetano

OPEN ACCESS

Correspondence:
Gabriela Franco da Rosa Caetano, DDS, MSc., Division of Oral and Maxillofacial Radiology, Department of Stomatology, School of Dentistry, University of São Paulo, São Paulo (SP), Brazil. Tel: 5535988681215; E-mail: gabrielafrc@usp.br/ gabrielafrc@hotmail.com

Received Date: *05 May 2026*
Accepted Date: *09 Jun 2026*
Published Date: *11 Jun 2026*

Citation:
Carvalho APR, Caetano GFR, Costa ALF, de Carvalho MO, Pinho KA, Junqueira JLC, et al. Association of Cone Beam CT Texture Parameters with Mandibular Bone Density and Structural Disorganization in Postmenopausal Women. WebLog J Dent Oral Disord. wjdod.2026. f1105. https://doi.org/10.5281/ zenodo.20951412

Abstract

Objectives: This study aimed to evaluate mandibular cortical index and texture analysis parameters derived from CBCT in women of different age groups and to explore their correlation.

Methods: A retrospective observational study was conducted on CBCT scans of 66 women, divided into two groups: Group A (32–50 years, n = 33) and Group B (51–76 years, n = 33). Computed Tomography Mandibular Index (CTMI) were measured at the mental foramen region, and texture analysis was performed using the gray-level co-occurrence matrix (GLCM) to extract eleven parameters. Statistical analyses included Student's t-test, Mann–Whitney U test, and Pearson/ Spearman correlation coefficients.

Results: The mean CTMI was 4.10 mm in Group A and 3.25 mm in Group B, indicating greater susceptibility to low BMD in group B. Group A exhibited higher AngScMom and InvDiffMom values, reflecting greater uniformity and homogeneity of trabecular structure. Group B showed higher Contrast, SumOfSqs, SumEntrp, Entropy, DifVarnc, and DifEntrp values, indicating increased variance, dispersion, and disorganization of gray-level intensities. Positive correlations were observed between CTMI and AngScMom and InvDiffMom, while negative correlations were found with Contrast, SumOfSqs, SumVarnc, SumEntrp, Entropy, DifVarnc, and DifEntrp. Patients with cortical bone thickness below 3 mm, indicative of osteoporosis, exhibited higher SumOfSqs and SumVarnc.

Conclusions: Computed Tomography Mandibular Index and texture analysis parameters are associated with bone mineral density and may serve as valuable, low-cost, and low-radiation screening tools.

Keywords: Cone Beam CT; Bone Mineral Density; Osteoporosis; Osteopenia; Texture Analysis

Introduction

Osteoporosis is defined as low bone mineral density characterized by altered microstructure, with a consequent increase in bone fragility and susceptibility to fracture [1, 2]. Bone loss has an early onset and is more pronounced in women [3] due to estrogen deficiency [4]. Bone mineral density (BMD) measurement by dual-energy x-ray absorptiometry (DXA) is the standard tool to assess the condition [5]. According to World Health Organization (WHO) [6], a T-score of -1.0 or higher is normal, a T-score between -1.0 and -2.5 is osteopenia, and a T-score of less than -2.5 indicates osteoporosis.

However, DXA remains costly and not widely accessible [7]. Alternative methods for screening patients with osteoporosis have been [8]. Pachêco-Pereira et al. (2019) [9], through a systematic review, investigated the use of dental imaging techniques to analyze trabecular bone structure

and identify systemic disorders, and found them to be useful for osteoporosis assessment. The mandibular cortical index (MCI) analyzed by panoramic radiography, for example, correlates with skeletal BMD measured by dual X-ray absorptiometry [10].

Cone-beam computed tomography (CBCT) is widely used for the qualitative and quantitative assessment of bone, providing dimensional accuracy, spatial resolution, grayscale values, and contrast [11]. CBCT images provide better visibility than panoramic radiographs and can be used to investigate mandibular indices [12]. Recent studies have shown that CBCT has great potential for analyzing osteoporosis due to the visibility of the MCI along its entire length [13], measurement of morphometric indices, radiographic density, and assessment of trabecular microstructure [7, 8].

A three-dimensional image is composed of voxels. Each voxel is represented by a set of coordinates with a specific value, which represents the gray level of the image [14]. Texture analysis (TA) is an image processing method that evaluates the heterogeneity of gray levels and spatial organization of the voxels in CBCT images [15, 16]. By analyzing texture parameters, it is possible to characterize and differentiate tissues, medullary bone changes [17], and bone microarchitecture [18]. Texture features are intrinsic image properties, including brightness, color, and size, which can be analyzed in terms of smoothness, roughness, regularity, or linearity [16].

Texture analysis (TA) was applied to head computed tomography (CT) and showed potential utility for osteoporosis diagnosis [19]. TA has also been used to evaluate changes in osteonecrotic bone pattern [18], dental implant stability [15], mandibular condyle analysis [16,17], and detection of furcal lesions [20].

Although several studies have explored the use of CBCT and panoramic radiographs to assess mandibular cortical indices and bone quality, no previous research has directly correlated gray-level co-occurrence matrix (GLCM), derived texture parameters from CBCT images with the Computed Tomography Mandibular Index (CTMI) in postmenopausal women. This correlation is particularly relevant because both measurements provide complementary information: CTMI reflects cortical bone thickness, while GLCM texture parameters describe trabecular organization and gray-level homogeneity. Establishing this relationship may enhance the diagnostic capability of CBCT as a non-invasive tool for detecting early microarchitectural alterations associated with reduced bone mineral density.

Therefore, this study aimed to evaluate the CTMI and TA parameters in women of different age groups, and to investigate their possible correlation as indicators of bone condition.

Materials and Methods

Patients

Ethical approval was obtained under protocol number 35869714.5.0000.5149. A retrospective observational study was conducted using CBCT images of women aged 32 to 50 years (G1: n = 33) and 51 to 76 years (G2: n = 33). The following factors were considered: age range at two levels - CBCT images of women aged 30 to 50 years and those aged 51 years or older (independent variable); cortical thickness and the texture analysis parameters (dependent variables).

Image acquisition

All CBCT scans were performed using an OP 300 Maxio cone-beam computed tomography unit (Instrumentarium Dental, Type BLD-NGEO-M, Serial No. IE1503469B, Tuusula, Finland) with a field of view (FOV) of 13 × 15 cm and a voxel size of 0.32 mm. CBCT scans of patients under 18 years of age and with poor image quality were excluded. Images containing filling materials or implants near the analyzed region were discarded due to the potential for interference with texture analysis.

The sample comprised a total of 66 female patients aged 32 to 76 years. The scans were divided into two groups: Group A – patients aged 32 to 50 years (n = 33); and Group B – patients aged 51 to 76 years (n = 33).

Image processing and analysis

All images were exported in Digital Imaging and Communications in Medicine (DICOM) format to OnDemand3D software (Cybermed Inc., Seoul, South Korea). The same window settings (brightness and contrast) were applied to the multiplanar reconstruction images to establish a uniform standard for all scans.

Mandibular cortical index

The morphometric measurements were performed by a dentomaxillofacial radiologist with more than five years of experience. For the quantitative evaluation, the axial and coronal CBCT images of the mandible were positioned at the central region of the mental foramen. The indices were evaluated according to the study by Brasileiro et al. (2017) [8], as follows:

- CTMI: Computed Tomography Mandibular Index, defined as the inferior cortical width of the mandible (Figure 1A).
- CTI (S): Computed Tomography Index (Superior), defined as the ratio of the inferior cortical width to the distance from the superior margin of the mental foramen to the inferior border of the mandible (Figure 1B).

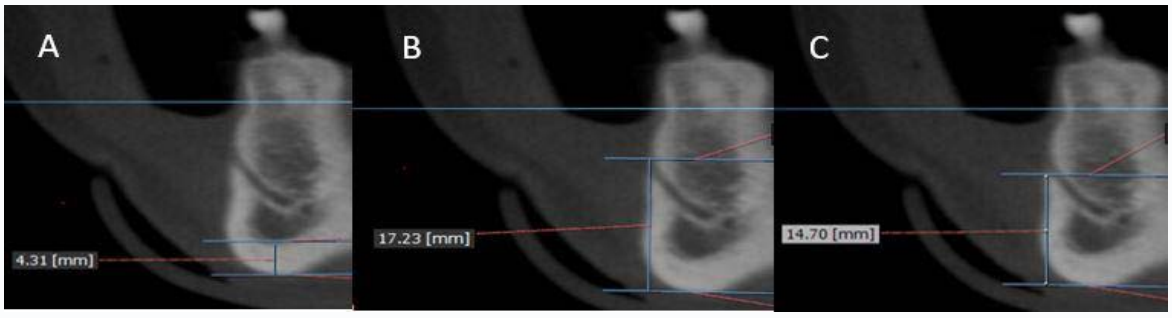

Figure 1: Tomographic images in the coronal plane showing the reference lines used for measurements: (A) CTMI; (B) CTI (S); and (C) CTI (I).

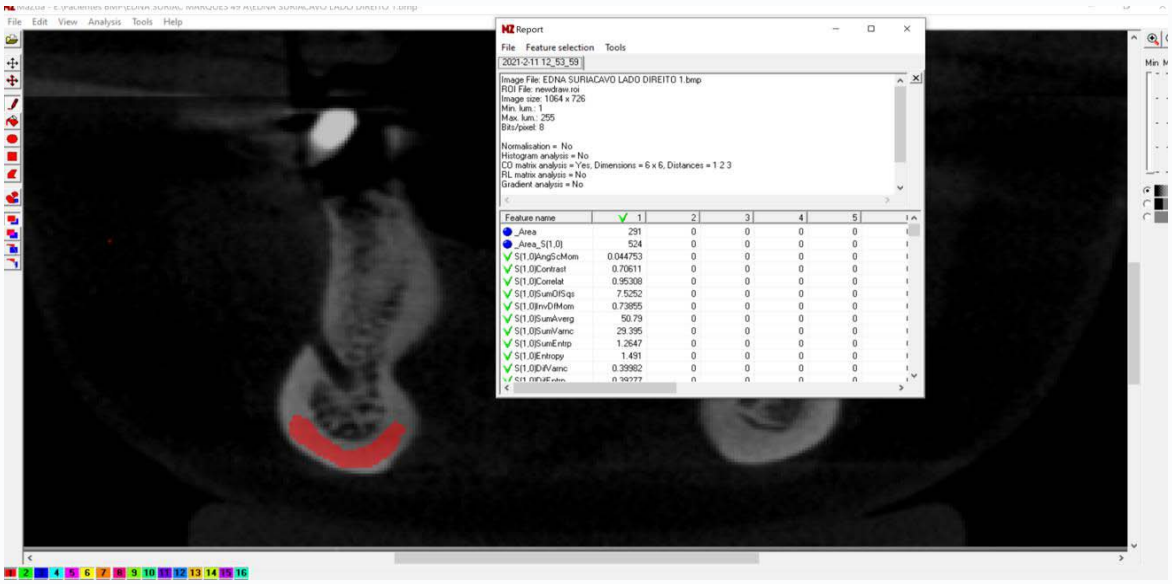

Figure 2: Tomographic images in the coronal plane. Texture parameter extraction performed using the MaZda software.

- CTI (I): Computed Tomography Index (Inferior), defined as the ratio of the inferior cortical width to the distance from the inferior margin of the mental foramen to the inferior border of the mandible (Figure 1C).

Texture analysis

Texture analysis provides an objective and quantitative evaluation of the distribution and relationships among the gray-level values in an image. It provides information about the spatial relationships between pixels within the region of interest (ROI), as defined by the operator. The GLCM tabulates the frequency of different combinations of pixel intensity values (gray levels) occurring in the image.Texture analysis was performed using a statistical approach through gray-level co-occurrence matrix (GLCM) analysis.

After accessing the image at the mental foramen region, three sequential 2D images with a thickness of 1 mm were generated. Three images were selected to create a segmented three-dimensional representation of the selected cortical area. These images were then converted to Bitmap format and transferred to MAZDA software, where the selected area was analyzed (Figure 2). Rectangular regions of interest (ROIs) measuring 1 mm were delineated and saved in bitmap format (.bmp) using OnDemand3D software (Cybermed Inc., Seoul, South Korea). MAZDA software (Mazda Research, Tokyo, Japan) was used to analyze the images in BMP format. The MaZda 4.60 software can make variations in the coordinates of the spatial relationship of the component elements of this matrix, thus determining the frequency of different information relating to the values of the analysed pixels [17].

Eleven texture parameters, as originally proposed by Haralick et al. (1973) [21], were used in this study, as follows: Angular Second Moment (ASM/AngScMom): measurement of image uniformity; Contrast: represents the amount of local variation in gray levels; Correlation (Correlat): linear dependency of gray levels between neighboring pixels; Sum of Squares (SumOfSqs): measures the dispersion of gray-level distribution relative to the mean; Inverse Difference Moment (IDM/InvDiffMom): measures image homogeneity (higher values indicate more uniformity); Sum Average (SumAverg): mean of the sum of gray levels in the GLCM; Sum Variance (SumVarnc): variance of the sum distribution of gray levels; Sum Entropy (SumEntrp): disorganization of the sum distribution of gray levels; Entropy: degree of disorder among pixels in the image; Difference Variance (DifVarnc): variance of the difference distribution of gray levels; and Difference Entropy (DifEntrp): disorder of the difference distribution of gray levels.

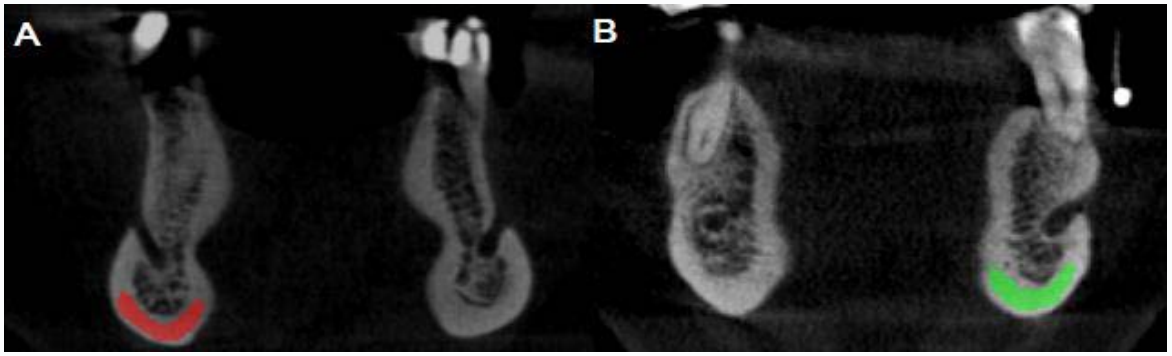

Figure 3: Tomographic images in the coronal plane. Regions of interest (ROIs) for pixel analysis. Pixels on the right side are shown in red (A), and those on the left side in green (B).

Table 1: Comparison between groups regarding age, CTMI, CTI (S) and CTI (I) (Student's t-test).

Variable	Group				p-value
	A (n=33)		B (n=33)		
	Mean (SD)	Median [Min;Max]	Mean (SD)	Median [Min;Max]	
Age (Years)	42,7 (5,24)	43,0 [32,0;50,0]	62,4 (6,44)	62,0 [51,0;76,0]	
CTMI	4,10 (0,79)	4,10 [2,85;6,00]	3,25 (0,80)	3,20 [1,65;5,10]	<0,001
CTI (S)	0,25 (0,05)	0,24 [0,18;0,40]	0,21 (0,05)	0,20 [0,10;0,30]	<0,001
CTI (I)	0,31 (0,06)	0,30 [0,22;0,51]	0,26 (0,06)	0,25 [0,12;0,39]	<0,001

Source: Author.

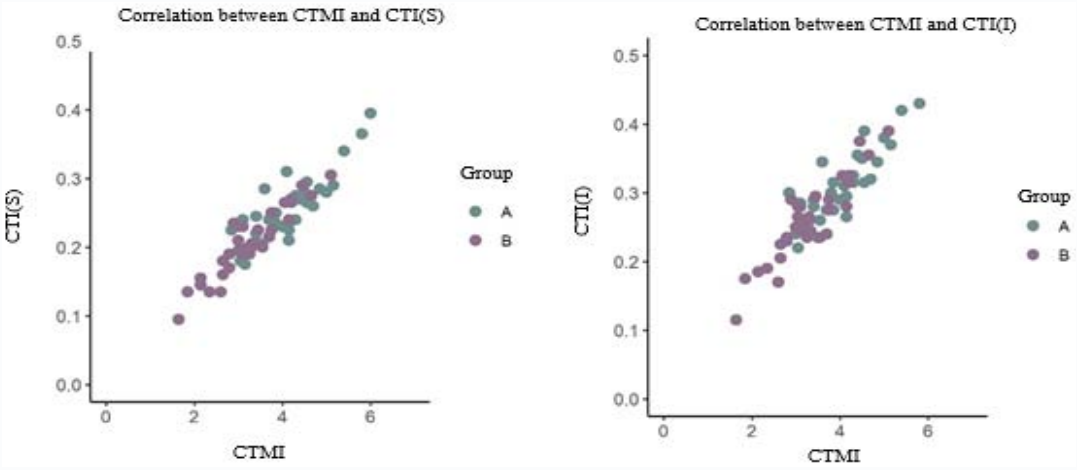

Figure 4: Scatter plots and Pearson correlation coefficients between the measurements CTMI, CTI(S) and CTI(I).

After transferring the images to MAZDA software, the region of interest (ROI) was acquired for pixel analysis. In the images, pixels on the right side were represented in red (Figure 3A) and those on the left side in green (Figure 3B). Each patient underwent six texture analyses (three on the right side and three on the left side of the mental foramen region). The acquired area in the study ranged from 215 to 343 pixels.

For pixel acquisition, the selection was performed across the entire inferior cortical region from the buccal to the lingual side, for subsequent extraction of texture parameters. After selecting the parameters, the analysis was conducted, and the data were tabulated in Microsoft Excel for statistical analysis.

Statistical analysis

An exploratory data analysis was performed by calculating descriptive statistics (mean, standard deviation, median, minimum, and maximum) and constructing graphs. Data normality was assessed using the Shapiro–Wilk test. Groups were compared using Student's t-test for morphometric indices and the Mann–Whitney U test for texture analysis parameters. For comparisons between groups in texture analysis, p-values were adjusted using the false discovery rate (FDR) method. Pearson's correlation coefficient was used to assess correlations between morphometric indices, while Spearman's correlation coefficient was applied to evaluate the relationship between morphometric indices, texture analysis parameters, and age. A significance level of 5% was adopted. Statistical analyses were performed using R software, version 3.6.2 (Copyright © 2019, The R Foundation for Statistical Computing).

Results

A total of 66 women aged 32 to 76 years participated in the study. These women were divided into two age groups: Group A, under 50 years old, and Group B, over 51 years old. The mean age of Group A was 42.7 years and Group B was 62.4 years, as shown in Table 1. This table also presents the comparison between the age groups regarding the morphometric indices. It is noted that the younger group exhibited higher values of CTMI (p-value < 0.001), CTI (S) (p-value < 0.001) and CTI (I) (p-value < 0.001).

Figure 4 shows the correlation between the morphometric indices evaluated: CTMI, CTI (S) and CTI (I). Correlation analysis was performed for the total sample of women as well as by age group. A strong correlation was observed between the CTMI, CTI (S) and CTI (I), both in the overall group and within each age group. The correlation coef Nficient ranges from –1 to 1, where values closer to either extreme indicate a stronger relationship between the two variables, whereas values closer to zero indicate a weaker linear correlation.

Texture analysis was evaluated in the directions S(1,0), S(0,1), S(1,1), S(1,-1), S(2,0), S(0,2), S(2,2), S(2,-2), S(3,0), S(0,3), S(3,3), and S(3,-3). Group A exhibited higher values of AngScMom and InvDfMom, whereas Group B showed higher values of Contrast, SumOfSqs, SumVarnc, SumEntrp, Entropy, DifVarnc, and DifEntrp, except for the directions S(3,0) and S(3,3). No statistically significant differences were observed between the groups for the Correlat and SumAverg parameters.

Table 2: Mean values of GLCM texture analysis in the directions S(0,1) (vertical), S(1,0) (horizontal), S(1,1) (45° diagonal), S(1,-1) (135° diagonal), S(3,0) (horizontal with a distance of 3), and S(3,3) (45° diagonal with a distance of 3), with values for Groups A and B, respectively.

Parameter	S(0,1) Vertical A	S(0,1) Vertical B	S(1,0) Horizontal A	S(1,0) Horizontal B	S(1,1) Diagonal 45° A	S(1,1) Diagonal 45° B	S(1,-1) Diagonal 135° A	S(1,-1) Diagonal 135° B	S(3,0) Horizontal A	S(3,0) Horizontal B	S(3,3) Diagonal 45° A	S(3,3) Diagonal 45° B
AngScMom	0,04 ± 0,03**	0,02 ± 0,01**	0,04 ± 0,03*	0,02 ± 0,01*	0,04 ± 0,03**	0,02 ± 0,01**	0,04 ± 0,02*	0,02 ± 0,01*	0,03 ± 0,02*	0,02 ± 0,01*	0,03 ± 0,02**	0,02 ± 0,01**
InvDfMom	0,62 ± 0,10**	0,54 ± 0,07**	0,62 ± 0,12*	0,54 ± 0,07*	0,56 ± 0,11**	0,47 ± 0,07**	0,55 ± 0,11**	0,47 ± 0,07**	0,48 ± 0,10**	0,40 ± 0,07**	0,41 ± 0,10*	0,34 ± 0,07*
Contrast	1,77 ± 1,61**	2,79 ± 1,54**	2,05 ± 1,81*	2,74 ± 1,22*	2,80 ± 2,46**	4,38 ± 2,26**	2,78 ± 2,29**	4,20 ± 2,29**	4,48 ± 3,62**	8,01 ± 5,51**	6,67 ± 5,83**	12,0 ± 8,88**
SumOfSqs	7,27 ± 4,86*	10,6 ± 5,84*	7,20 ± 4,84*	10,6 ± 5,96*	7,17 ± 4,84*	10,5 ± 5,88*	7,13 ± 4,80*	10,5 ± 5,90*	6,42 ± 4,30**	10,0 ± 6,15**	6,43 ± 4,45**	9,91 ± 5,54**
SumVarnc	27,3 ± 18,2*	39,8 ± 22,4*	26,8 ± 17,9*	39,7 ± 23,2*	25,9 ± 17,3*	37,8 ± 22,1*	25,7 ± 17,3*	37,9 ± 22,2*	21,2 ± 14,1*	32,1 ± 20,8*	19,0 ± 12,7*	27,6 ± 16,6*
SumEntrp	1,23 ± 0,13*	1,32 ± 0,09*	1,23 ± 0,13*	1,32 ± 0,10*	1,22 ± 0,13*	1,30 ± 0,09*	1,22 ± 0,13*	1,30 ± 0,09*	1,18 ± 0,13*	1,27 ± 0,10*	1,14 ± 0,12*	1,22 ± 0,09*
Entropy	1,57 ± 0,24**	1,76 ± 0,15**	1,58 ± 0,26*	1,76 ± 0,15*	1,63 ± 0,25**	1,82 ± 0,15**	1,64 ± 0,24*	1,82 ± 0,15*	1,68 ± 0,23**	1,86 ± 0,16**	1,69 ± 0,23**	1,87 ± 0,15**
DifVarnc	0,82 ± 0,75**	1,26 ± 0,73**	0,95 ± 0,79*	1,22 ± 0,53*	1,22 ± 1,07**	1,91 ± 1,06**	1,22 ± 1,03*	1,82 ± 1,05*	1,93 ± 1,67**	3,44 ± 2,47**	2,34 ± 2,06**	4,70 ± 3,95**
DifEntrp	0,48 ± 0,11**	0,58 ± 0,08**	0,50 ± 0,13*	0,58 ± 0,08*	0,55 ± 0,13**	0,66 ± 0,08**	0,56 ± 0,12**	0,65 ± 0,09**	0,64 ± 0,13**	0,75 ± 0,11**	0,69 ± 0,13**	0,82 ± 0,11**
Correlat	0,87 ± 0,04	0,86 ± 0,05	0,86 ± 0,06	0,85 ± 0,06	0,80 ± 0,07	0,77 ± 0,08	0,79 ± 0,07	0,78 ± 0,08	0,65 ± 0,12°	0,58 ± 0,13°	0,49 ± 0,14°	0,39 ± 0,19°
SumAverg	59,3 ± 12,0	60,1 ± 9,72	59,3 ± 11,9	60,1 ± 9,75	59,3 ± 12,0	60,1 ± 9,74	59,3 ± 11,9	60,1 ± 9,75	59,1 ± 11,8	60,0 ± 9,76	59,0 ± 11,8	60,0 ± 9,75

** p < 0,001; * p < 0,01; ° p < 0,05; No symbol: p ≥ 0,05.

Table 3: Spearman correlation coefficient of the CTMI measure with TA in different directions – Overall Group.

Parameter	S(1,0)	S(0,1)	S(1,1)	S(1,-1)	S(2,0)	S(0,2)	S(2,2)	S(2,-2)	S(3,0)	S(0,3)	S(3,3)	S(3,-3)
AngScMom	0,477*	0,470*	0,492*	0,487*	0,490*	0,458*	0,500*	0,474*	0,504*	0,438*	0,460*	0,444*
Contrast	-0,463*	-0,518*	-0,520*	-0,551*	-0,523*	-0,545*	-0,555*	-0,557*	-0,548*	-0,539*	-0,549*	-0,526*
Correlat	0,019	0,145	0,16	0,197	0,158	0,202	0,313*	0,353*	0,329*	0,2	0,305*	0,363*
SumOfSqs	-0,497*	-0,500*	-0,502*	-0,499*	-0,499*	-0,508*	-0,510*	-0,506*	-0,509*	-0,507*	-0,516*	-0,507*
InvDfMom	0,434*	0,509*	0,494*	0,523*	0,476*	0,512*	0,529*	0,545*	0,527*	0,478*	0,506*	0,463*
SumAverg	-0,232	-0,23	-0,23	-0,232	-0,226	-0,232	-0,232	-0,228	-0,219	-0,236	-0,229	-0,218
SumVarnc	-0,494*	-0,498*	-0,494*	-0,484*	-0,488*	-0,486*	-0,465*	-0,442*	-0,473*	-0,468*	-0,465*	-0,423*
SumEntrp	-0,449*	-0,459*	-0,476*	-0,447*	-0,447*	-0,443*	-0,459*	-0,404*	-0,432*	-0,443*	-0,438*	-0,375*
Entropy	-0,493*	-0,505*	-0,511*	-0,519*	-0,505*	-0,511*	-0,511*	-0,501*	-0,515*	-0,484*	-0,482*	-0,459*
DifVarnc	-0,458*	-0,508*	-0,518*	-0,537*	-0,510*	-0,536*	-0,578*	-0,559*	-0,535*	-0,536*	-0,568*	-0,561*
DifEntrp	-0,471*	-0,513*	-0,521*	-0,542*	-0,520*	-0,537*	-0,564*	-0,561*	-0,550*	-0,536*	-0,526*	-0,539*

*Significant at the 5% level.

In the directions S(3,0) and S(3,3), Group A presented higher Correlat values. For these two directions, no significant differences were observed between the groups for the SumAverg parameter either. Table 2 presents the mean values for the texture analysis directions S(0,1) (vertical), S(1,0) (horizontal), S(1,1) (45° diagonal), S(1,-1) (135° diagonal), S(3,0) (horizontal with a distance of 3), and S(3,3) (45° diagonal with a distance of 3). The first four directions were selected because they correspond to the most commonly evaluated orientations in GLCM texture analyses reported in the literature. S(3,0) and S(3,3) were additionally included as they exhibited distinct values, allowing for the assessment of relevant variations at larger distances.

Regarding the correlation between the texture analysis parameters and the CTMI index, it can be inferred that in the directions S(1,0), S(0,1), S(1,1), S(1,-1), S(2,0), S(0,2), and S(0,3), a positive correlation was observed between AngScMom and InvDfMom and the CTMI index, while a negative correlation was found between Contrast, SumOfSqs, SumVarnc, SumEntrp, Entropy, DifVarnc, and DifEntrp and the CTMI index. This correlation was observed for the total group of women and for Group B. The correlation between the CTMI index and the texture analysis parameters was not significant in Group A.

In the directions S(2,2), S(3,0), and S(3,3), a positive correlation between Correlat and CTMI was also observed in the total group. Similarly, in the directions S(2,-2) and S(3,-3), a positive correlation between Correlat and CTMI was found in both the total group and Group B. Tables 3, 4, and 5 show the Spearman correlation coefficient of the CTMI measure with TA in the different directions for the overall group, Group A, and Group B, respectively.

Table 6 presents the comparison between two groups formed based on the cortical measure (CTMI< 3 and CTMI ≥ 3) regarding the texture analysis parameters in the S(1,0) direction, considering only age group B. It can be observed that the CTMI < 3 group shows lower AngScMom and InvDfMom, and higher Contrast, SumOfSqs, SumVarnc, SumEntrp, Entropy, DifVarnc, and DifEntrp, with $p < 0.001$ for the SumOfSqs and SumVarnc parameters.

Discussion

The development of an efficient and cost-effective method for early detection of osteoporosis is essential [22]. Therefore, this study aimed to evaluate the Computed Tomography Mandibular Index and texture analysis in women of different age groups, and to assess their possible correlation. The mean age of group A was 42.7 years, and that of group B was 62.4 years. The mandibular cortical index was higher in group A than in group B. In the texture analysis, group A showed higher values of AngScMom (uniformity) and InvDfMom (homogeneity). A positive correlation was observed

Table 4: Spearman correlation coefficient of the CTMI measure with TA in different directions – Group A.

Parameter	S(1,0)	S(0,1)	S(1,1)	S(1,-1)	S(2,0)	S(0,2)	S(2,2)	S(2,-2)	S(3,0)	S(0,3)	S(3,3)	S(3,-3)
AngScMom	0,253	0,233	0,255	0,215	0,206	0,253	0,254	0,212	0,217	0,249	0,208	0,211
Contrast	-0,263	-0,221	-0,241	-0,251	-0,238	-0,278	-0,3	-0,284	-0,26	-0,28	-0,29	-0,291
Correlat	0,105	0,117	0,117	0,129	0,148	0,153	0,21	0,224	0,216	0,131	0,237	0,299
SumOfSqs	-0,293	-0,31	-0,306	-0,299	-0,276	-0,351*	-0,329	-0,328	-0,27	-0,373*	-0,309	-0,295
InvDfMom	0,214	0,236	0,222	0,24	0,203	0,26	0,259	0,319	0,246	0,25	0,273	0,279
SumAverg	-0,161	-0,159	-0,16	-0,159	-0,151	-0,159	-0,144	-0,153	-0,15	-0,169	-0,127	-0,148
SumVarnc	-0,3	-0,316	-0,3	-0,295	-0,283	-0,345*	-0,317	-0,3	-0,233	-0,378*	-0,312	-0,277
SumEntrp	-0,229	-0,257	-0,27	-0,245	-0,213	-0,284	-0,279	-0,213	-0,192	-0,306	-0,255	-0,164
Entropy	-0,275	-0,233	-0,257	-0,25	-0,222	-0,245	-0,258	-0,225	-0,238	-0,263	-0,243	-0,203
DifVarnc	-0,26	-0,221	-0,253	-0,235	-0,269	-0,28	-0,32	-0,313	-0,292	-0,287	-0,279	-0,3
DifEntrp	-0,264	-0,218	-0,236	-0,258	-0,237	-0,274	-0,306	-0,304	-0,26	-0,278	-0,275	-0,283

*Significant at the 5% level.

Table 5: Spearman correlation coefficient of the CTMI measure with TA in different directions – Group B.

Parameter	S(1,0)	S(0,1)	S(1,1)	S(1,-1)	S(2,0)	S(0,2)	S(2,2)	S(2,-2)	S(3,0)	S(0,3)	S(3,3)	S(3,-3)
AngScMom	0,479*	0,388*	0,469*	0,503*	0,558*	0,389*	0,471*	0,500*	0,549*	0,373*	0,388	0,439*
Contrast	-0,487*	-0,476*	-0,490*	-0,614*	-0,562*	-0,461*	-0,507*	-0,559*	-0,556*	-0,415*	-0,513*	-0,502*
Correlat	-0,098	0,029	-0,053	0,16	0,065	0,085	0,123	0,364*	0,312	0,169	0,16	0,367*
SumOfSqs	-0,503*	-0,503*	-0,509*	-0,511*	-0,510*	-0,515*	-0,491*	-0,496*	-0,501*	-0,479*	-0,496*	-0,491*
InvDfMom	0,409*	0,448*	0,439*	0,527*	0,539*	0,434*	0,491*	0,511*	0,570*	0,373*	0,429*	0,442*
SumAverg	-0,293	-0,292	-0,292	-0,293	-0,283	-0,292	-0,299	-0,291*	-0,269	-0,292	-0,304	-0,277
SumVarnc	-0,489*	-0,505*	-0,519*	-0,482*	-0,483*	-0,501*	-0,465*	-0,426*	-0,478*	-0,476*	-0,448*	-0,397*
SumEntrp	-0,443*	-0,449*	-0,526*	-0,446*	-0,463*	-0,465*	-0,497*	-0,404*	-0,430*	-0,482*	-0,455*	-0,377*
Entropy	-0,529*	-0,520*	-0,531*	-0,568*	-0,562*	-0,509*	-0,502*	-0,527*	-0,542*	-0,477*	-0,443*	-0,453*
DifVarnc	-0,500*	-0,460*	-0,474*	-0,613*	-0,519*	-0,446*	-0,528*	-0,567*	-0,519*	-0,409*	-0,509*	-0,527*
DifEntrp	-0,496*	-0,460*	-0,495*	-0,587*	-0,561*	-0,451*	-0,522*	-0,569*	-0,542*	-0,437*	-0,473*	-0,513*

*Significant at the 5% level.

Table 6: Comparison between groups formed based on the cortical measure in age group B (>50 years) regarding texture analysis in the S(1,0) direction.

Variable	Group B				p-value
	CTMI<3 (N=22)		CTMI≥3 (N=44)		
	Mean (SD)	Median [Min;Max]	Mean (SD)	Median [Min;Max]	
AngScMom	0.02 (0.01)	0.02 [0.01;0.03]	0,03 (0,01)	0.03 [0.01;0.06]	0.002
Contrast	3.51 (1.49)	3.73 [1.08;6.71]	2,36 (1,02)	1.97 [0.68;4.71]	0.002
Correlat	0.86 (0.07)	0.87 [0.67;0.95]	0,85 (0,07)	0.84 [0.69;0.94]	0.237
SumOfSqs	15.1 (8.27)	12.2 [4.98;34.9]	8,38 (3,32)	8.37 [3.03;17.6]	**<0.001**
InvDfMom	0.50 (0.07)	0.51 [0.39;0.64]	0.55 (0.07)	0.56 [0.43;0.73]	0.011
SumAverg	63.5 (9.89)	65.4 [49.0;78.3]	58.4 (9.43)	56.5 [45.9;82.2]	0.053
SumVarnc	56.8 (32.4)	45.9 [16.9;136]	31.2 (12.9)	30.9 [10.6;67.7]	**<0.001**
SumEntrp	1.38 (0.11)	1.39 [1.19;1.56]	1.29 (0.09)	1.30 [1.11;1.46]	0.001
Entropy	1.85 (0.16)	1.89 [1.60;2.12]	1.71 (0.14)	1.70 [1.36;2.00]	0.001
DifVarnc	1.57 (0.65)	1.56 [0.45;2.79]	1.05 (0.46)	0.90 [0.37;2.51]	0.001
DifEntrp	0.63 (0.09)	0.65 [0.43;0.76]	0.56 (0.07)	0.55 [0.38;0.70]	0.002

between the AngScMom and InvDfMom parameters and the CTMI index, whereas Contrast, SumOfSqs, SumVarnc, SumEntrp, Entropy, DifVarnc, and DifEntrp parameters showed a negative correlation with the CTMI index. Patients with cortical bone thickness below 3 mm exhibited higher SumOfSqs and SumVarnc.

In the study conducted by Brasileiro et al. (2017) [8], bone mineral density was correlated with age. The mean ages were 55.6 years in the normal group, 57.5 years in the osteopenia group, and 62.4 years in the osteoporosis group [8]. In the present study, the mean age was 42.7 years in group A and 62.4 years in group B. Since bone densitometry was not performed, women up to 50 years of age were included in group A, and older than 51 years were included in group B. The selection criteria was based on the fact that Type 1 osteoporosis

(postmenopausal) typically occurs approximately 10 to 15 years after menopause, most commonly between 50 and 70 years of age [23], and this osseous condition predominantly affects individuals older than 50 years [24].

The majority of postmenopausal women with osteoporosis have bone loss related to estrogen deficiency [4], wich impairs bone tissue turnover and promotes skeletal bone degeneration [22]. Estrogen binds with estrogen receptor to promote the expression of osteoprotegerin (OPG), suppress the action of nuclear factor-κβ ligand (RANKL), inhibit osteoclast formation and bone resorptive activity, and increase the secretion of IL-1, IL-6, and tumor necrosis factor (TNF) [4]. In addition, the trabecular structure in women tends to exhibit a thinner and more linear morphology, making it more susceptible to changes during bone remodeling [16].

The mandibular cortical index correlates with bone mineral density and is well established in the literature as a diagnostic indicator of osteoporosis [8, 10, 11, 22, 25, 26]. Several studies correlating mandibular cortical measurements with DXA have reported lower linear values in osteoporotic individuals [1, 8, 10, 11, 27]. Therefore, in the present study, the mandibular cortical index was correlated with texture analysis in premenopausal and postmenopausal women.

Resorption in osteoporotic patients occurs primarily in the Haversian and Volkmann canals, which supply blood to the cortical bone [26]. The cortical height in the mental foramen region correlates with lumbar spine BMD in postmenopausal women, supporting the measurement of this region [28]. An MCI value below 3.4 mm indicates a 3.9-fold increased risk of developing osteoporosis [22], and values under 3.0mm may represent a threshold for predicting low bone mineral density, suggesting referral for DXA assessment [8, 22, 27]. In the present study, the mean mandibular cortical width was 4.10 mm in group A and 3.25 mm in group B, indicating a predisposition to the disease in group B. One-third of the women in Group B can be classified as having osteoporosis, as the MCI measurement was below 3 mm. In the study conducted by Brasileiro et al. (2017) [8], the mean CTMI values were 3.68 and 2.93 in patients with osteopenia and osteoporosis, respectively. Similarly, in the study by Gungor et al. (2016) [25], the mean CTMI values were 3.42 and 2.76 in patients with osteopenia and osteoporosis, respectively. In this study, Group B also presented lower values of the Inferior and Superior Computed Tomography Index, similar to the findings reported by Brasileiro et al. (2017) [8].

This study represents one of the first attempts to address the methodology of evaluating the inferior mandibular cortex through CBCT texture analysis to identify low bone mineral density. With texture analysis, changes in bone patterns [18], characterization and differentiation of various tissues based on their textural properties can be detected [17]. In the study conducted by Kawashima et al. (2019) [19], CT texture analysis was compared with bone densitometry, and statistically significant differences were observed in the bilateral sphenoid triangles, mandibular condyles, and clivus.

In the texture analysis, statistically significant differences were found among the evaluated parameters, suggesting an alteration in the cortical bone structure between the groups. Group A showed higher AngScMom and InvDiffMom values, indicating greater uniformity and homogeneity, with better organization and distribution of the bone trabeculae. The secondary angular moment is a parameter that represents the uniformity of the gray-level distribution in the image; meaning that images with a lower number of gray levels exhibit greater uniformity. The inverse difference moment measures the smoothness (homogeneity) of the gray-level distribution; when contrast is low, the InvDiffMom value is high.

In the texture analysis, group B showed higher values of Contrast, SumOfSqs, SumEntrp, Entropy, DifVarnc, and DifEntrp, indicating greater dispersion, variance, and gray-level disorganization, consistent with disrupted trabecular architecture and a predisposition to osteopenia/osteoporosis.

These textural alterations directly reflect the underlying microarchitectural changes in bone tissue. Parameters such as Contrast and Entropy are sensitive to irregularities in gray-level distribution, indicating higher trabecular disorganization and increased cortical porosity, features typically observed in osteopenic and osteoporotic bone. In contrast, ASM and InvDfMom express uniformity and homogeneity of the voxel intensity distribution, which are associated with greater trabecular connectivity and a denser, more compact cortical structure. Therefore, the reduction in ASM and IDM values observed in older women suggests a loss of trabecular continuity and increased cortical porosity, reinforcing the potential of texture analysis to capture subtle structural deterioration that precedes measurable decreases in bone mineral density.

Contrast represents the amount of local variation in gray levels; a high value may indicate the presence of edges, noise, or roughness within the image. Entropy measures the degree of disorder among pixels in the image; higher entropy values indicate greater variation in gray-level intensities. Similar results were reported by Kavitha et al. (2015) [29], in which the p-values for AngScMom, Contrast, InvDiffMom, SumEntrp, Entropy, and DifVarnc were below 0.05, indicating significant differences between osteoporotic and normal patients with respect to lumbar spine and femoral neck BMD. This demonstrates that GLCM texture analysis is strongly correlated with systemic bone condition, showing that the changes present in the spine and femur are reflected in the mandibular cortical microstructure [29]. High values for the parameters contrast, entropy, sum entropy, sum of squares, and angular second moment indicate greater disorder and a lack of uniformity in pixel distribution, suggesting areas affected by osteolytic processes [18].

No statistically significant differences were found between Groups A and B for the parameters Correlat and SumAverg. Similar to the study conducted by Kawashima et al. (2019) [19], in which the Correlat parameter derived from computed tomography showed no significant differences between patients with normal bone mineral density and those with osteoporosis in the sphenoid triangles, mandibular condyles, and clivus region. In contrast, the study conducted by Kavitha et al. (2015) [29] reported significant differences in the Correlat parameter between normal and osteoporotic patients. However, that study used panoramic radiographs, in which bone structures and other anatomical features tend to overlap. The Correlat parameter represents the degree of interdependence between image pixels, with higher values indicating greater pixel interdependence [17].

Unlike previous studies using panoramic images, the present analysis focuses on cortical texture extracted from CBCT, which offers higher spatial resolution and is not affected by superimposition. This may explain why our correlations between CTMI and texture parameters were stronger than those reported in panoramic-based

studies.

According to the correlation analysis between the CTMI index and texture analysis, evaluated across the directions S(1,0), S(0,1), S(1,1), S(1,–1), S(2,0), S(0,2), and S(0,3), a positive correlation was observed for the AngScMom and InvDfMom parameters, indicating that higher CTMI values are associated with greater uniformity and homogeneity of the trabecular bone. Whereas a negative correlation was observed between the CTMI index and the parameters Contrast, SumOfSqs, SumVarnc, SumEntrp, Entropy, DifVarnc, and DifEntrp, indicating that lower CTMI values are associated with greater variation and disorganization in gray levels, as well as increased dispersion of the gray-level distribution relative to the mean.

Cortical bone thicknesses below 3 mm, indicating osteoporosis, were associated with higher Contrast, SumOfSqs, SumVarnc, SumEntrp, Entropy, DifVarnc, and DifEntrp. Entropy is directly related to bone structural organization; higher entropy values reflect reduced tissue uniformity and increased variability in gray-level intensities [17]. Elevated contrast values are indicative of non-homogeneous structures [15], exhibiting greater noise and reduced uniformity, which in turn reflect increased variation and decreased similarity among gray-level intensities [17].

Patients exhibiting a Computed Tomography Mandibular Index (CTMI) below 3 mm demonstrated significant differences ($p < 0.001$) in Sum of Squares (SumOfSqs) and Sum Variance (SumVarnc) parameters, reflecting substantial alterations in cortical bone architecture. These elevated values indicate increased textural heterogeneity, characterized by greater dispersion and variability in gray-level intensity distributions within the bone matrix, indicating a more irregular and porous cortical structure with structural disorganization. These findings suggest that the association between morphometric indices and texture-analysis parameters may represent a promising tool for screening low bone mineral density. This aligns with the results reported by Kavitha et al. (2015) [29], in which the combination of textural features and MCW yielded superior discriminatory performance for identifying osteoporosis based on femoral neck and lumbar spine BMD.

The limitations of this study included the small sample size, the absence of bone densitometry (the gold standard for diagnosing osteoporosis), and the fact that the women evaluated were relatively healthy. Future studies should include a larger sample size and incorporate comparison with the gold-standard examination (bone densitometry) to determine whether the parameter value ranges are reliable for classifying patients as normal, osteoporotic, or osteopenic. Considering the loss of resolution that occurs when converting 2D images to Bitmap, a 3D texture analysis using the texture parameters is recommended.

In conclusion, CBCT mandibular cortical thickness and texture-analysis parameters are associated with bone mineral density, demonstrating their potential as screening tools for osteopenia/osteoporosis. The mean mandibular cortical index (MCI) was 4.10 mm in women under 50 years of age (Group A) and 3.25 mm in women over 51 years (Group B), indicating a higher predisposition to the disease in Group B.

In texture analysis, Group A exhibited higher AngScMom and InvDiffMom values, indicating greater uniformity and homogeneity of the trabecular structure, whereas Group B displayed higher values of Contrast, SumOfSqs, SumEntrp, Entropy, DifVarnc, and DifEntrp, reflecting increased dispersion, variance, and disorganization of gray-level intensities.

In the correlation between MCI and texture analysis, a positive association was observed for the AngScMom and InvDfMom parameters, indicating that higher CTMI values are associated with greater uniformity and homogeneity of the trabecular bone. Conversely, the CTMI index exhibited a negative correlation with the parameters Contrast, SumOfSqs, SumVarnc, SumEntrp, Entropy, DifVarnc, and DifEntrp, indicating that lower CTMI values are associated with greater variation and disorganization of gray levels, as well as increased dispersion in the gray-level distribution relative to the mean. Patients in Group B with cortical bone thickness below 3 mm, indicative of osteoporosis, exhibited higher SumOfSqs and SumVarnc.

Morphometric measurements and texture analysis from tomographic images may provide a valuable tool for assessing bone status and for the screening of osteopenia and osteoporosis, as well as for identifying patients at risk of low bone mineral density (BMD), given the lower radiation exposure associated with this imaging modality. In addition to being low-cost and low-radiation, this approach could facilitate population-wide screening and help reduce public health expenses related to the treatment and prevention of these conditions.

References

1. Mostafa RA, Arnout EA, Abo El-Fotouh MM. Feasibility of cone beam computed tomography radiomorphometric analysis and fractal dimension in assessment of postmenopausal osteoporosis in correlation with dual X-ray absorptiometry. *Dentomaxillofac Radiol.* 2016; 45(7): 20160212. https://doi.org/10.1259/dmfr.20160212
2. Porter JL, Varacallo MA. Osteoporosis. In: StatPearls [Internet]. Treasure Island (FL): StatPearls Publishing; 2025 Jan–. Available from: https://www.ncbi.nlm.nih.gov/books/NBK441901/
3. Alswat KA. Gender disparities in osteoporosis. *J Clin Med Res.* 2017; 9(5): 382–387. https://doi.org/10.14740/jocmr2970w
4. Cheng CH, Chen LR, Chen KH. Osteoporosis due to hormone imbalance: an overview of the effects of estrogen deficiency and glucocorticoid overuse on bone turnover. *Int J Mol Sci.* 2022; 23(3): 1376. https://doi.org/10.3390/ijms23031376
5. Haseltine KN, Chukir T, Smith PJ, Jacob JT, Bilezikian JP, Farooki A. Bone mineral density: clinical relevance and quantitative assessment. *J Nucl Med.* 2021; 62(4): 446–454. https://doi.org/10.2967/jnumed.120.256180
6. World Health Organization. Prevention and Management of osteoporosis. Geneva: WHO; 2003.
7. Guerra ENS, Almeida FT, Bezerra FV, Figueiredo PTDS, Silva MAG, De Luca Canto G, Pachêco-Pereira C, Leite AF. Capability of CBCT to identify patients with low bone mineral density: a systematic review. *Dentomaxillofac Radiol.* 2017; 46(8): 20160475. https://doi.org/10.1259/dmfr.20160475
8. Brasileiro CB, Chalub LLFH, Abreu MHNG, Barreiros ID, Amaral TMP, Kakehasi AM, Mesquita RA. Use of cone beam computed tomography in identifying postmenopausal women with osteoporosis. *Arch Osteoporos.* 2017; 12(1): 26. https://doi.org/10.1007/s11657-017-0314-7
9. Pachêco-Pereira C, Almeida FT, Chavda S, Major PW, Leite A, Guerra ENS. Dental imaging of trabecular bone structure for systemic disorder screening: a systematic review. *Oral Dis.* 2019; 25(4): 1009–1026. https://doi.org/10.1111/odi.12950
10. Munhoz L, Morita L, Nagai AY, Moreira J, Arita ES. Mandibular cortical index in the screening of postmenopausal at low mineral density risk: a

systematic review. *Dentomaxillofac Radiol*. 2021; 50(4): 20200514. https://doi.org/10.1259/dmfr.20200514

11. Poiana IR, Dobre R, Popescu RI, Pituru SM, Bucur A. Utility of cone-beam computed tomography in the detection of low bone mass: a systematic review. *J Clin Med*. 2023; 12(18): 5890. https://doi.org/10.3390/jcm12185890

12. Koseoglu Secgin C, Gulsahi A, Yavuz Y, Kamburoglu K. Comparison of mandibular index values determined from standard panoramic versus cone beam computed tomography reconstructed images. *Oral Surg Oral Med Oral Pathol Oral Radiol*. 2019; 127(3): 257–264. https://doi.org/10.1016/j.oooo.2018.10.007

13. Alonso MB, Vasconcelos TV, Lopes LJ, Watanabe PC, Freitas DQ. Validation of cone-beam computed tomography as a predictor of osteoporosis using the Klemetti classification. *Braz Oral Res*. 2016; 30(1): e263. https://doi.org/10.1590/1807-3107BOR-2016.vol30.0073

14. Oliveira MS, Fernandes PT, Avelar WM, Santos SLM, Castellano G, Li LM. Texture analysis of computed tomography images of acute ischemic stroke patients. Braz J Med Biol Res. 2009; 42(11): 1076–1079.

15. Costa ALF, de Souza Carreira B, Fardim KAC, Nussi AD, da Silva Lima VC, Miguel MMV, Jardini MAN, Santamaria MP, de Castro Lopes SLP. Texture analysis of cone beam computed tomography images reveals dental implant stability. *Int J Oral Maxillofac Surg*. 2021. https://doi.org/10.1016/j.ijom.2021.04.009

16. Nussi AD, de Castro Lopes SLP, De Rosa CS, Gomes JPP, Ogawa CM, Braz-Silva PH, Costa ALF. In vivo study of cone beam computed tomography texture analysis of mandibular condyle and its correlation with gender and age. *Oral Radiol*. 2023; 39(1): 191–197. https://doi.org/10.1007/s11282-022-00620-3

17. Moraes MB, Costa NCQ, Silva GYSD, Costa FC, Raldi FV, Lopes SLPC. Unveiling degenerative bone changes in the condyle: a texture analysis approach using cone-beam computed tomography. *Acta Cir Bras*. 2025; 40: e401325. https://doi.org/10.1590/acb401325

18. Queiroz PM, Fardim KC, Costa ALF, Matheus RA, Lopes SLPC. Texture analysis in cone-beam computed tomographic images of medication-related osteonecrosis of the jaw. Imaging Sci Dent. 2023; 53(2): 109–115. https://doi.org/10.5624/isd.20220202

19. Kawashima Y, Fujita A, Buch K, Li B, Qureshi MM, Chapman MN, Sakai O. Using texture analysis of head CT images to differentiate osteoporosis from normal bone density. *Eur J Radiol*. 2019; 116: 212–218. https://doi.org/10.1016/j.ejrad.2019.05.009

20. Gonçalves BC, de Araújo EC, Nussi AD, Bechara N, Sarmento D, Oliveira MS, et al. Texture analysis of cone-beam computed tomography images assists the detection of furcal lesion. *J Periodontol*. 2020; 91: 1159–1166. https://doi.org/10.1002/JPER.19-0477

21. Haralick RM. Texture features for image classification. *IEEE Trans Syst Man Cybern*. 1973; SMC-3(6): 610–621.

22. Triantafyllopoulos G, Mitsea A, Rontogianni A, Korres D. Osteoporosis screening using dental panoramic radiographs and age at menarche. *Diagnostics (Basel)*. 2023; 13(5): 881. https://doi.org/10.3390/diagnostics13050881

23. Keen MU, Barnett MJ, Anastasopoulou C. Osteoporosis in females. In: StatPearls [Internet]. Treasure Island (FL): StatPearls Publishing; 2025 Jan–. Available from: https://www.ncbi.nlm.nih.gov/books/NBK559156/

24. Kanis JA, McCloskey EV, Johansson H, Oden A, Melton LJ, Khaltaev N. A reference standard for the description of osteoporosis. *Bone*. 2008; 42(3): 467–475.

25. Gungor E, Yildirim D, Cevik R. Evaluation of osteoporosis in jaw bones using cone beam CT and dual-energy X-ray absorptiometry. *J Oral Sci*. 2016; 58: 185–194. https://doi.org/10.2334/josnusd.15-0609

26. Taguchi A, Tanaka R, Kakimoto N, Morimoto Y, Arai Y, Hayashi T, Kurabayashi T, Katsumata A, Asaumi J; Japanese Society for Oral and Maxillofacial Radiology. Clinical guidelines for the application of panoramic radiographs in screening for osteoporosis. *Oral Radiol*. 2021; 37(2): 189–208. https://doi.org/10.1007/s11282-021-00518-6

27. Kim OS, Shin MH, Song IH, Lim IG, Yoon SJ, Kim OJ, Lee YH, Kim YJ, Chung HJ. Digital panoramic radiographs are useful for diagnosis of osteoporosis in Korean postmenopausal women. *Gerodontology*. 2016; 33(2): 185–192. https://doi.org/10.1111/ger.12134

28. Naitoh M, Kurosu Y, Inagaki K, Katsumata A, Noguchi T, Ariji E. Assessment of mandibular buccal and lingual cortical bones in postmenopausal women. *Oral Surg Oral Med Oral Pathol Oral Radiol Endod*. 2007; 104(4): 545–550. https://doi.org/10.1016/j.tripleo.2007.04.034

29. Kavitha MS, An SY, An CH, Huh KH, Yi WJ, Heo MS, Lee SS, Choi SC. Texture analysis of mandibular cortical bone on digital dental panoramic radiographs for the diagnosis of osteoporosis in Korean women. *Oral Surg Oral Med Oral Pathol Oral Radiol*. 2015; 119(3): 346–356. https://doi.org/10.1016/j.oooo.2014.11.009